International Journal of Mechanical and Production Engineering Research and Development (IJMPERD)
ISSN (P): 2249-6890; ISSN (E): 2249-8001
Vol. 9, Issue 2, Apr 2019, 569-578

PLASTIC BUCKLING OF AXIALLY COMPRESSED CYLINDERS: CORRELATION BETWEEN THEORY AND EXPERIMENTS

O. IFAYEFUNMI

Fakulti Teknologi Kejuruteraan Mekanikal dan Pembuatan, Universiti Teknikal Malaysia Melaka, Durian Tunggal, Melaka, Malaysia

ABSTRACT

For an axially compressed cylinder, early experiments revealed that the experimental load is about 30% below the theoretical load. This paper aims to provide better comparison between experimental and theoretical data for cylinders subjected to axial compression through the appropriate experimental procedure. Ten cylinders (five steel and five aluminum) were made using different joining techniques. Two cylindrical geometric parameters were considered, they are : (i) thinness ratio (i. e., radius-to-thickness ratio, R/t) of 18.66 - 21.42, and (ii) slenderness ratio (i. e., length-to-radius ratio, L/R) of 1 - 5. All the specimens were manufactured from 2 mm flat plate. Comparison of results obtained from theory, simulation (ABAQUS FE) and experiments reveals that there is a good agreement in the magnitude of the load carrying capacity and deformed shape of the cylinders. The corresponding ratios varied here from 1.01 to 1.05 (steel cylinders), and from0.99 to 1.02 (aluminum cylinders). But the goodness of the comparison is observed to depend strongly on the material properties used and the clamping arrangement adopted during the experimentation.

KEYWORDS: Buckling, Cylindrical Shell, ABAQUS, Axial Compression, Numerical/Theoretical Prediction & Boundary Conditions

Received: Jan 25, 2019; **Accepted**: Feb 15, 2019; **Published**: Mar 19, 2019; **Paper Id.**: IJMPERDAPR201956

Original Article

INTRODUCTION

Thin-walled circular cylinders are used mainly as structural components in many engineering practice such as aerospace, civil, mechanical, pressure vessel, marine and offshore industries. For example, thick cylinders typically with low radius-to-thickness ratio, R/t, are commonly used in marine, offshore and ocean engineering application such as pipelines, pressure vessels etc. In many applications, the thickness of the cylinder is constant and the cylinder is subjected to various loading conditions, i. e., external pressure, internal pressure, axial compression, torsion and combination of one or more individual loads. For such application, the cylinder is prone to failure by buckling which has been a subject of interest over the past year, especially when subjected to axial compression. This explains the reasons for numerous research work for this shell geometry. Comprehensive review of the buckling behavior of cylindrical shells are presented in [1-5]. For cylinder under axial compression, earlier experiments revealed that the load carrying capacity for real cylinders underestimate the theoretical predicted values by about 30%. This discrepancy between theoretical prediction of the buckling load of cylinder as compared to experimentally obtained value has been over time attributed to the sensitivity of the cylinder to imperfections/defects. The reason for this major difference in both theoretical buckling load and experimental data has attracted numerous research in the area of imperfection sensitivity of the cylinder. Review of past work on the imperfection sensitivity of cylinders can be found in [6]. Studies on axially compressed cylinder with initial

geometric imperfections are presented in [7-9]. Whilst, [10-12] covers imperfect cylinder subjected to axial compression with non-uniform axial length. Investigation into the imperfection sensitivity of an axially compressed cylinder with non-uniform loading can be found in [13-17]. Surprisingly, the problem is far from being solved. In fact, this problem has been predicted to be one of the last classical problems in homogenous isotropic structural mechanics where it remains difficult to achieve good agreement between theoretical buckling load and experiments. The motivation for this present work originates from the conclusion of Ifayefunmi [18] where comparison was made between experimental data and theoretical/numerical predictions for load carrying capacity of relatively short mild steel cylinders subjected to axial compression. Ifayefunmi [18] examines this long standing problem of isotropic structural mechanics (i. e., discrepancies in buckling load of cylinder subjected to axial compression) and highlights some important facts on how this problem could be solved. It was revealed in [18] that good agreement between theoretical/numerical predictions and experimental finding on the buckling loads for thick steel cylinders (with radius-to-thickness ratio, R/t, ranging from 25 to 100) could be achieved. However, these experimental data were limited.

This paper aims to complement the preliminary results presented in [18] by providing further experiments on the buckling behavior of short and thick mild steel cylinders subjected to axial compression. In addition, it is intended to extend the scope of the work to different material such as aluminum cylinder. Cylinders were joined together using different joining techniques. For a mild steel cylinder, Tungsten Inert Gas (TIG) welding process was employed. Whilst, for aluminum cylinder, the seam between two neighboring longitudinal free edges of the cylinder were glued together using epoxy resin. The wall thickness of the specimen was constant at 2 mm. For steel cylinders, the radius-to-thickness ratio, R/t, of the cylinder was varied from 18.66 to 21.42. Whereas, for aluminum cylinders, the length-to-radius ratio, L/R, of the cylinder was varied from 1 to 5, while the radius-to-thickness ratio, R/t, of the cylinder was kept at 25. These radius-to-thickness ratios were chosen because they are typical geometry commonly used for pipelines and pressure vessels components. Comparisons of prediction of load carrying capacity were made between experimental buckling load, theoretical prediction and numerical calculations. Numerical calculations were obtained using ABAQUS FE software, [19].

BACKGROUND

Let us examine a circular cylinder having diameter, D, radius, R and uniform wall thickness, t, with axial length, L, as depicted in Figure 1a. The cylinder is assumed to be under axial compression as sketched in Figure 1b. Generally, the buckling behaviour of such cylinder under axial compression depends on its geometry parameters such as radius R, thickness t and length L, its material properties (i. e., elastic modulus E and yield stress σ_{yp}), the size and type of imperfections in its geometry, the ends support/boundary conditions and the pattern of loading.

Cylindrical shells geometry parameters are mostly expressed in terms of ratio, viz: (i) thinness ratio (i. e., radius-to-thickness ratio, R/t), and (ii) slenderness ratio (i. e., length-to-radius ratio, L/R). Cylinders can be classified either as thin-walled or thick-walled structures based on the thinness ratio. For this classification to be made, the following assumptions must be considered, they are: (i) radius-to-thickness ratio, R/t >10 is thin-walled structures, and (ii) radius-to-thickness ratio, R/t < 10 is thick-walled structures.

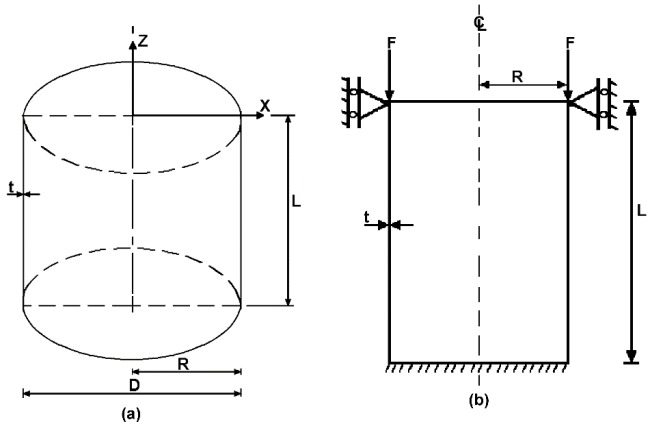

Figure 1: Illustration of Geometry of Analysed Cylinder (a), Cylinder under Axial Compression (b)

Generally, when a circular thin-walled cylinder is under uniform axial compression, the surface of a high-quality cylindrical shell suddenly and dramatically changes from the original shape into a wave-like which is referred to as buckling mode. For cylinders under axial compression, depending on the ratio of radius-to-thickness, the following buckling modes can be experienced, they are: (i) axisymmetric collapse mode for relatively thick cylinder with low value of radius-to-thickness ratio. This failure mode is characterized by a single or multiple bulge around the circumference with respect to the axis as shown in Figure 2a - 2b, and (ii) asymmetric bifurcation mode for thinner cylinder with high value of radius-to-thickness ratio, characterized by the development of alternatively inward and outward displacement of the cylinder wall with several full waves around the circumference, and usually several waves up the height as presented in Figure 2c – 2e. However, this paper will be devoted to collapse behaviour of relatively thick cylinder with low value of radius-to-thickness ratio. For relatively thick cylinder, the reference buckling load, F_{ref}, is expressed as the load needed to cause yielding of the cylinder and it is given by:

$$F_{ref} = \pi D t \sigma_{yp} \quad (1)$$

Where

F_{ref} = Reference plastic buckling load

σ_{yp} = Yield stress

D = Cylinder diameter

t = Cylinder wall thickness.

Although, the buckling mode is primarily influenced by the radius-to-thickness ratio, but it can also depend on the ratio of the length to the radius of the cylinder, L/R. For example, for relatively long cylinder, the buckling mode changes from axisymmetric collapse mode to Euler buckling mode.

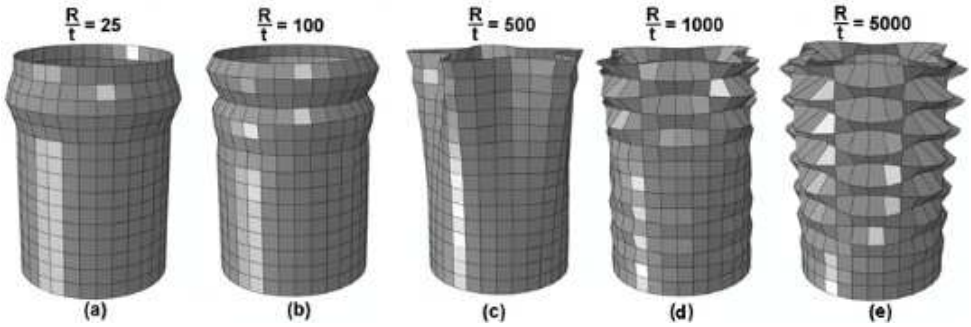

Figure 2: Computed Axisymmetric Collapse Mode of Failure (a & b) and Asymmetric Bifurcation Mode of Failure (c, d & e) for Cylinder with Different Thinness Ratio

MATERIAL AND METHODS

A total of ten cylinders were manufactured and tested under axial compression. Five mild steel cylinders having different thinness ratio, R/t, with radius, R = 37.32, 38.64, 40, 41.41 and 42.82 mm and another five aluminium cylinders having different slenderness ratio (L/R ≈ 1, 2, 3, 4 and 5). The steel cylinders are 2 mm in thickness and 115.95 mm in height. Specimens were designated as CS1 – CS5 (i. e., cylinder made from steel material). Whilst, the aluminium cylinders were assumed to have nominal thickness, t = 2 mm and nominal diameter, D = 105 mm. The axial lengths for all aluminium cylinders were varied between 50 mm and 250 mm. Specimens were designated as CA1 – CA5. Prior to experimental work, the mechanical properties of the 2mm rectangular plate used in this study were obtained using tensile testing. The flat tensile specimen were designed according to British Standard (BS EN 10002-1: 2001), [20]. During the cutting process, the tensile test coupons were cut in the same cutting direction employed for loading the cylinders under axial compression. The tensile coupons were subjected to uni-axial tensile test using INSTRON testing machine until they failed. The rate of loading was 1.0 mm/min. The average material data obtained for the uni-axial tensile test is given in Table 1. The tensile specimens were not stress relieved at any stage of their manufacture.

Table 1: Material Properties Obtained from Tested Tensile 2 mm Tensile Coupons (E = Young's Modulus, UTS = Ultimate Tensile Strength)

	E (GPa)	Upper Yield (MPa)	UTS (MPa)	Poisson's Ratio
Steel	219.82	369.9	408.2	0.30
Aluminium	81.557	144.0	146.9	0.33

After the material testing, abrasive water jet machine was used to cut the rectangular flat plates to the desired dimension. Subsequently, the flat plate is rolled into a cylindrical form with the help of conventional rolling machine (see Figure 3 of [21] for more details). After the rolling process, the seam between the two neighbouring longitudinal free edges of the steel cylinder is welded using Tungsten Inert Gas (TIG) welding process. The choice of Tungsten Inert Gas (TIG) was made because of the wall thickness of the steel cylinder. However, because of the complication in welding aluminium as compared to mild steel, the seam between the two neighbouring longitudinal free edges of the rolled specimens were joined together using epoxy resin. To obtain effective gluing process, 5 mm overlap is machined on each adjacent edge of the cylinder using a milling machine. Then, the epoxy was applied to the overlap section. Afterwards, the specimen is hold together using a clamp until the epoxy harden.

RESULTS AND DISCUSSIONS

Prior to testing, manufacture-induced imperfections were taken into consideration. A number of measurements (i. e., wall thickness, diameter and axial length) were taken on all cylindrical specimens. Firstly, Ultrasonic thickness measurement gauge was used to measure the wall thickness at eleven (11) equal points along the axial meridian of the cylinder. This was then repeated along the circumference of the cylinder at 36 degrees apart, producing 11 x 10 = 110 measuring points. The nominal thickness t_{nom}, average thickness t_{ave}, minimum thickness t_{min}, maximum thickness t_{max} and the standard deviation t_{std} for all cylinders are provided in Table 2. Secondly, the digital Vernier caliper was used to measure the inner and outer diameters of the specimens. Measurements were taken at five equally spaced diameters at the top and bottom ends respectively. The average measured mid-surface diameter for all specimens are given in Table 3. Thirdly, the digital Vernier caliper was used to measure the axial lengths of the cylinders at eleven equal points. The measured average axial lengths are also presented in Table 3.

Table 2: Measured Wall Thickness for Tested Cylindrical Specimens

	t_{nom}	t_{min}	t_{max}	t_{ave}	t_{std}
	mm				
CS1	2.0	1.98	2.04	2.008	0.0166
CS2	2.0	1.98	2.04	2.011	0.0169
CS3	2.0	1.98	2.04	2.011	0.0184
CS4	2.0	1.98	2.04	2.012	0.0147
CS5	2.0	1.98	2.03	1.999	0.0151
CA1	2.0	1.97	1.99	1.978	0.0051
CA2	2.0	1.97	2.00	1.986	0.0105
CA3	2.0	1.97	2.00	1.990	0.0108
CA4	2.0	1.97	2.00	1.991	0.0087
CA5	2.0	1.97	2.00	1.988	0.0122

Table 3: Measured Average Diameter at Top and Bottom and Axial Length for Tested Cylindrical Specimens

Note: $\overline{D}$ ≡ Average Mid-Surface Diameter

	$\overline{D_{top}}$	$\overline{D_{bottom}}$	L_{ave}	$\overline{D_{top}}/t_{ave}$	$L_{ave}/\overline{D_{top}}$
	(mm)				
CS1	74.54	74.60	116.39	37.12	1.56
CS2	77.02	77.87	116.26	38.30	1.51
CS3	79.99	80.08	116.38	39.77	1.45
CS4	82.99	82.66	116.39	41.27	1.40
CS5	85.68	85.74	116.32	42.86	1.36
CA1	107.25	107.50	49.84	54.22	0.46
CA2	107.48	107.53	101.77	54.12	0.95
CA3	107.75	107.87	150.85	54.15	1.40
CA4	107.63	107.61	200.48	54.06	1.86
CA5	107.01	107.39	249.67	53.83	2.33

After all the measurements were carried out, all the cylindrical models were subjected to axial compression using INSTRON machine. Cylinders were placed between the INSTRON machine platens without any clamping plates. This testing arrangement and procedures are the same as previously described in [18]. View of steel cylinder CS4 in between the INSTRON platen and ready to be tested is depicted in Figure 3.

Figure 3: Typical Experimental Arrangements of Cylinder before Testing (CS4 Model)

It is expected that the platen of the INSTRON machine will help to provide the desirable boundary condition, i. e., the support plate was assumed to restrict all displacement and rotational degree of freedom (d. o. f) at the bottom end of the cylinder. The same boundary conditions were assumed at the top end of the cylinder except for displacement d. o. f in the axial direction. This is to enable the application of axial compressive force. However, it is realistically impossible to obtain this boundary condition without rotation, but numerical result has shown that the influence of rotation on the magnitude of load carrying capacity of cylinder under axial compression is marginal, [22]. During the experiments, compression load was applied at one end of the cylinder along the axial direction. The rate of loading was kept at 1.0 mm/min – same loading rate employed in the material testing. The axial force and the resulting compression extension were recorded by the INSTRON. Figure 4 present the plot of axial load versus compression extension for steel cylinders (Figure 4a) and aluminium cylinders (Figure 4b). It is apparent that all curves follow a similar trend. Surprisingly, from Figure 4a, four different regions were observed from the curve, they are: (i) nearly linear portion from 0 - 120 kN, (ii) a transition region at about 120 kN, (iii) an increase in axial force from 120 kN to the collapse force, and (iv) a region after the collapse load. The first region corresponds to the elastic region of the structure where the deformation is temporary. In the second region, the structure is seen to be undergoing yielding – a transition point from elastic to plastic deformation. While, in the third region, the structure can be said to be undergoing strain hardening within the plastic region. Finally, in the fourth region, it is the post collapse region of the structures. It is apparent from Figure 4b, unlike the steel cylinder, the curves are nearly linear up to the collapse load. This can be attributed to a typical behaviour of aluminium material where there is no well-defined yield point. All cylinder models failed suddenly with the axial load drop as given in Table 4.

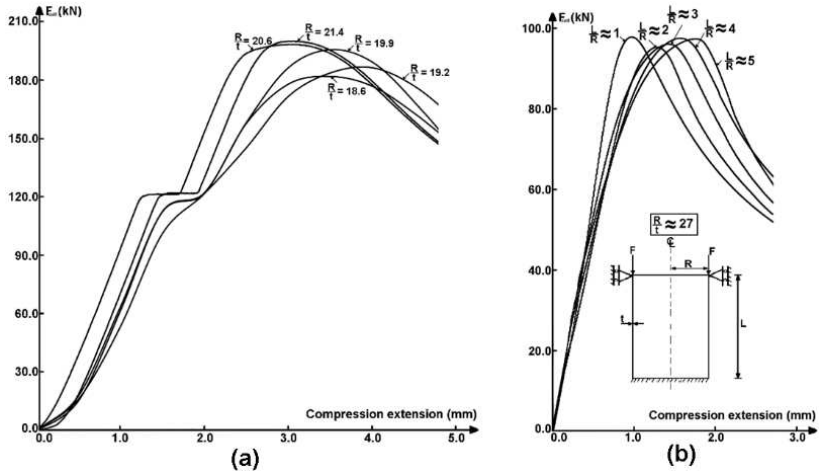

Figure 4: Plot of Load Versus Compression Extension for Steel Cylinders (a) and Aluminium Cylinders (b)

Table 4: Comparison of Experimental Buckling Loads and Numerical/Theoretical Predictions for Cylinders under Axial Compression

Models	$\bar{R}/t$	L/R	F_{exptl}	$F_{theortl}$	F_{ABAQUS}	$F_{exptl}/F_{theortl}$
			(kN)			
CS1	18.56	3.11	182.09	173.94	174.01	1.05
CS2	19.15	3.00	186.97	179.99	180.06	1.04
CS3	19.89	2.90	196.36	186.93	186.94	1.05
CS4	20.63	2.80	198.49	193.95	193.99	1.02
CS5	21.43	2.71	200.17	199.04	199.06	1.01
CA1	25.0	0.93	97.96	95.84	95.51	1.02
CA2	25.0	1.89	95.40	96.13	95.96	0.99
CA3	25.0	2.80	96.20	96.69	96.34	0.99
CA4	25.0	3.73	97.63	96.56	96.20	1.01
CA5	25.0	4.67	97.50	96.05	93.74	1.02

Figure 5 depicts the photograph of collapsed cylinders after testing. It can be observed here that all cylinders have an axisymmetric bulge at the region where the load was applied (i. e., top ends). This failure mode can be attributed to the influence of excessive plastic straining at the top ends of the cylinders.

To establish the goodness of the testing procedure adopted in this work, comparison was made between experimentally obtained results and theoretical reference load to cause yield of the cylinders as in Eq. 1. The average upper yield (Table 1), average thickness (Table 2) and average mid-surface diameter (Table 3) were used. The theoretical predicted collapse load for the cylindrical specimens is given in column 5 of Table 4. From Table 4, it is apparent that the theoretical reference load predicts the magnitude of buckling load in close agreement to that of the experimental results. For the all cylinder models, the theoretical predictions underestimate the experimental collapse load except for aluminium cylinders, CA2 and CA3. The ratio ranges from -1 to +5. Also, it can be noticed from Table 4 that increasing the length-to-radius ratio has little or no effect on the buckling of cylinder within the range covered in this paper, i. e., cylinder that fails within the elastic-plastic range ($R/t = 25$ and $1 \leq L/R \leq 5$). These results agree with theory – see (Eq. 1) where the length of the cylinder is clearly omitted in determining the theoretical reference load to cause failure of the cylinders. Although, this may not be valid for relatively long the cylinder where the buckling mode changes from axisymmetric collapse mode to Euler column buckling mode. In addition, this might not be generally true for the cylinder which fails within the elastic range. Hence, a further experimental and numerical analysis within the elastic behaviour will be encouraged.

Figure 5: Photograph of All Cylinders after Testing

Finally, numerical predictions based on the same geometry and material properties used in theoretical calculation were carried out. The same boundary conditions employed during experimentation was used for the ensuing numerical calculation. The specimens were modelled using four-node three-dimensional doubly curved shell elements with six degree of freedom (S4R). The material is modelled as elastic perfectly-plastic. Non-linear static analysis was carried out using the modified Riks method algorithm which is implemented in ABAQUS. The ensuing numerical calculations are given in column 6 of Table 4. From Table 4, the experimental and numerical results are seen to be in agreement. In addition, there is good visual comparison of deformed shape for both numerical analysis and experiment as exemplified for steel cylindrical model (CS1) in Figure 6.

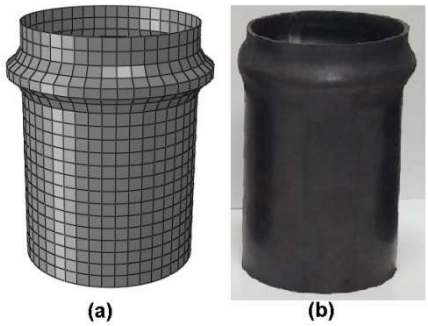

Figure 6: View of FE Simulated Deformed Shape (a) and Experimental Collapsed Shape (b) for Steel Cylinder CS1 with Approximately the Same Deformed Pattern

CONCLUSIONS

Theoretical/numerical and experimental results on the buckling behaviour of steel and aluminum cylinders subjected to axial compression have been presented. Generally, it is apparent from this piece of work that there is very good agreement between the magnitude of collapse load given by theory, simulation (ABAQUS) and experiment for all the cases of radius-to-thickness ratio, R/t, and length-to-radius ratio, L/R, considered. For steel cylinders, it has been found that the ratio of experimental/theoretical buckling loads varied between 1.01 and 1.05. Whilst for aluminum cylinders, the ratio ranges from 0.99 and 1.02. These results complement the preliminary results reported in Ref. [18], where it was mentioned that the influence of the manufacturing process is not significant. In addition, these results also validate and establish the appropriateness of the experimental procedure proposed in both pieces of work for buckling of axially compressed

cylinder. However, this may not be applicable to other geometries. More study into other geometry (i. e., cones) would be well justified. Finally, to obtain good agreement between experimental and theoretical prediction, these observations need to be made here. First, exact material data of the specimens must be used. And, second, the clamping arrangement employed during experiment must be made simple as adopted in this work.

ACKNOWLEDGEMENTS

Special thanks to Universiti Teknikal Malaysia Melaka (UTeM) and the Ministry of Education Malaysia under Fundamental Research Grant Scheme (FRGS/2018/FTKMP-CARE/F00386) for the financial support.

REFERENCES

1. *Teng, J. G., Rotter, J. M. (2004). Buckling of thin shells. In: Teng JG, Rotter JM, editors. Buckling of thin metal shells. London: Spon Press; p. 1-41..*
2. *Southwell, R. V. (1914). On the general theory of elastic stability. Philosophical Transaction of the Royal Society, 213, 187-202.*
3. *Teng, J. G. (2004). Cylindrical shells under axial compression. In: Teng JG, Rotter JM, editors. Buckling of thin metal shells. London: Spon Press; p. 42-87.*
4. *Singer, J., Arbocz, J., and Weller, T. (2002). Buckling Experiment – Experimental Methods in Buckling of Thin-Walled Structures. Vol. 2, New York: John Wiley & Sons Inc.*
5. *Blachut. J. (2014). Experimental Perspective on the Buckling of Pressure Vessel Components. Applied Mechanics Review, 66, 011003-1 – 011003-24.*
6. *Ifayefunmi, O., Blachut, J. (2018). Imperfection Sensitivity: A Review of Buckling Behavior of Cones, Cylinders, and Domes. Journal of Pressure Vessel Technology, Transactions of the ASME, 140, 050801-1-050801-8.*
7. *Amazigo, J. C., Budiansky, B. (1972). Asymptotic formulas for the buckling stresses of axially compressed cylinders with localized or random axisymmetric imperfections. Journal of Applied Mechanics, 93, 179–184.*
8. *Sunitha, K. R., & Jacob, B. (2015). Dynamic Buckling Of Steel Water Tank Under Seismic Loading. International Journal of Civil Engineering (IJCE) ISSN (P), 2278-9987.*
9. *Hutchinson, J., Muggeridge, D., Tennyson, R. (1971). Effect of local axisymmetric imperfection on the buckling behaviour of circular cylindrical shell under axial compression. AIAA Journal, 9, 48–52.*
10. *Khamlichi, A., Bezzazi, M., Limam, A. (2004). Buckling of elastic cylindrical shells considering the effect of localized axisymmetric imperfections. Thin-Walled Structures, 42, 1035–1047.*
11. *Blachut, J. (2010). Buckling of axially compressed cylinders with imperfect length. Computers and Structures, 88, 365–374.*
12. *Blachut, J. (2015). Buckling of cylinders with imperfect length. Journal of pressure vessel technology, 137, 011203-1–011203-7.*
13. *Friedrich, L., Reimerdes, H. G. (2013). Imperfection sensitivity of circular cylindrical shells of varying length subjected to axial compression. In: 54th AIAA/ASME/ASCE/AHS/ASC structures, structural dynamics and materials conference; Boston, MA.*
14. *Cai, M., Holst, J. M. F. G, Rotter, J. M. (2002). Buckling strength of thin cylindrical shells under localised axial compression. In: Proceeding of the 15th ASCE Engineering Mechanics Conference; New York, p. 99-100.*

15. *Krasovsky, V. (1993). Nonlinear effects in behaviour of cylindrical shells under nonuniform axial compression, Experimental Results. In: Proceedings of the 2nd International Conference on Nonlinear Mechanics; Beijing, p. 245–248.*
16. *Kriegesmann, B., Hilburger, M. W., Rolfes, R. (2012). The effects of geometric and loading imperfections on the response and lower-bound buckling load of a compression-loaded cylindrical shell. In: Proceedings of the 53rd AIAA/ASME/ASCE/AHS/ASC Structures, Structural Dynamics and Material Conference; Honolulu, Hawail.*
17. *Libai, A., Durban, D. (1977). Buckling of cylindrical shells subjected to nonuniform axial loads. Journal of Applied Mechanics, Transactions of the ASME, 44, 714-720.*
18. *Song, C. Y., Teng, J. G., Rotter, J. M. (2004). Imperfection sensitivity of thin elastic cylindrical shells subjected to partial axial compression. International Journal of Solids and Structures, 41, 7155–7180.*
19. *Ifayefunmi, O. (2016). Buckling behaviour of axially compressed cylindrical shells: Comparison of theoretical and experimental data. Thin-walled structures, 98, 558-564.*
20. *Hibbitt, Karlsson, and Sorensen Inc. (2006). ABAQUS – Theory and Standard User's Manual Version 6.3. USA: Pawtucket, RI, 02860-4847.*
21. *BS EN 10002-1. (2001). Tensile testing of Metallic Materials, Part (1), Method of test at ambient temperature. London, UK: British Standard Institute.*
22. *Ifayefunmi, O. (2016). The effect of axial crack on the buckling behaviour of axially compressed cylinders. International Journal of Mechanical and Mechatronics Engineering, 16, 12-17.*
23. *Ifayefunmi, O., Kadmin, A. F., Chang, K. L., Aziz, A. (2018). Influence of boundary condition on the buckling of axially compressed cones and cylinders. International Journal of Mechanical Engineering Technology, 9, 1106-1116.*